

# Development of GPC2-directed chimeric antigen receptors using mRNA for pediatric brain tumors

Jessica B Foster <sup>1,2,3</sup>, Crystal Griffin,<sup>3</sup> Jo Lynne Rokita <sup>3,4,5</sup>, Allison Stern,<sup>3</sup> Cameron Brimley,<sup>5</sup> Komal Rathi,<sup>3,4</sup> Maria V Lane,<sup>1</sup> Samantha N Buongervino,<sup>1</sup> Tiffany Smith,<sup>3</sup> Peter J Madsen,<sup>3,5</sup> Daniel Martinez,<sup>6</sup> Alberto Delaidelli,<sup>7</sup> Poul H Sorensen,<sup>7</sup> Robert J Wechsler-Reya,<sup>8</sup> Katalin Karikó,<sup>9</sup> Phillip B Storm,<sup>3,5,10</sup> David M Barrett,<sup>11</sup> Adam C Resnick,<sup>3,5</sup> John M Maris <sup>1,2</sup>, Kristopher R Bosse<sup>1,2</sup>

**To cite:** Foster JB, Griffin C, Rokita JL, *et al.* Development of GPC2-directed chimeric antigen receptors using mRNA for pediatric brain tumors. *Journal for ImmunoTherapy of Cancer* 2022;**10**:e004450. doi:10.1136/jitc-2021-004450

Accepted 27 August 2022

## ABSTRACT

**Background** Pediatric brain tumors are the leading cause of cancer death in children with an urgent need for innovative therapies. Glypican 2 (GPC2) is a cell surface oncoprotein expressed in neuroblastoma for which targeted immunotherapies have been developed. This work aimed to characterize GPC2 expression in pediatric brain tumors and develop an mRNA CAR T cell approach against this target.

**Methods** We investigated GPC2 expression across a cohort of primary pediatric brain tumor samples and cell lines using RNA sequencing, immunohistochemistry, and flow cytometry. To target GPC2 in the brain with adoptive cellular therapies and mitigate potential inflammatory neurotoxicity, we used optimized mRNA to create transient chimeric antigen receptor (CAR) T cells. We developed four mRNA CAR T cell constructs using the highly GPC2-specific fully human D3 single chain variable fragment for preclinical testing.

**Results** We identified high GPC2 expression across multiple pediatric brain tumor types including medulloblastomas, embryonal tumors with multilayered rosettes, other central nervous system embryonal tumors, as well as definable subsets of highly malignant gliomas. We next validated and prioritized CAR configurations using *in vitro* cytotoxicity assays with GPC2-expressing neuroblastoma cells, where the light-to-heavy single chain variable fragment configurations proved to be superior. We expanded the testing of the two most potent GPC2-directed CAR constructs to GPC2-expressing medulloblastoma and high-grade glioma cell lines, showing significant GPC2-specific cell death in multiple models. Finally, biweekly locoregional delivery of 2–4 million GPC2-directed mRNA CAR T cells induced significant tumor regression in an orthotopic medulloblastoma model and significantly prolonged survival in an aggressive orthotopic thalamic diffuse midline glioma xenograft model. No GPC2-directed CAR T cell related neurologic or systemic toxicity was observed.

**Conclusion** Taken together, these data show that GPC2 is a highly differentially expressed cell surface protein on multiple malignant pediatric brain tumors that can be targeted safely with local delivery of mRNA CAR T cells, laying the framework for the clinical translation of GPC2-directed immunotherapies for pediatric brain tumors.

## WHAT IS ALREADY KNOWN ON THIS TOPIC

⇒ GPC2 is an oncoprotein highly expressed in neuroblastoma and other cancers with low expression in normal tissues, making it an attractive candidate for immunotherapeutic approaches. Prior work has shown potent efficacy of GPC2-directed antibody-drug conjugates and DNA-based CAR T cell constructs in neuroblastoma. However, the efficacy of targeting GPC2 expressed on pediatric brain tumors with CAR T cells has not yet been explored.

## WHAT THIS STUDY ADDS

⇒ A comprehensive analysis of GPC2 expression across a diverse cohort of pediatric brain tumors revealed enriched expression in embryonal brain tumor histotypes as well as a subset of malignant gliomas. GPC2-directed CAR T cells created with mRNA showed tumor specific cytotoxicity in medulloblastoma and high-grade glioma *in vitro* and *in vivo* preclinical models. This work establishes the proof-of-concept efficacy of GPC2-directed CAR T cells in a subset of malignant pediatric brain tumors and the framework to further develop GPC2-directed immunotherapies for children with lethal CNS tumors.

## HOW THIS STUDY MIGHT AFFECT RESEARCH, PRACTICE OR POLICY

⇒ As CNS tumors are the leading cause of pediatric cancer death, testing novel therapies is imperative to improving long-term outcomes for these children. There have been encouraging early clinical trial results for CAR T cell therapy for pediatric CNS tumors, however the development of new immunotherapeutic targets is desperately needed. This study should motivate the design of additional GPC2 CAR efficacy and safety studies across several brain tumor preclinical models with an ultimate goal of clinical translation.

## BACKGROUND

Immunotherapy has recently developed into a major pillar of cancer therapy.<sup>1</sup> Chimeric antigen receptor (CAR) T cells offer targeted



© Author(s) (or their employer(s)) 2022. Re-use permitted under CC BY-NC. No commercial re-use. See rights and permissions. Published by BMJ.

For numbered affiliations see end of article.

## Correspondence to

Dr Jessica B Foster; fosterjb@chop.edu

T cell killing by combining the specificity of an antibody with the stimulatory signals of cytotoxic T cells.<sup>2</sup> CAR T cell therapy has provided dramatic success in leukemias and lymphomas<sup>3–5</sup> with tisagenlecleucel becoming the first U.S. Food and Drug Administration (FDA)-approved cellular therapy product.<sup>6</sup> This achievement has prompted similar investigations for solid tumors but without significant clinical success to date.<sup>7</sup> Developing effective CAR T cell therapy for solid tumors has many challenges related to difficulty finding appropriate target antigens, the suppressive tumor microenvironment, T cell dysfunction, and poor CAR T cell trafficking.<sup>7</sup> Among brain tumors, CAR T cell therapy remains in its infancy, with a handful of adult clinical trials showing minimal to transient success,<sup>8–10</sup> and trials in pediatric brain tumors only just beginning but with promising early results.<sup>11,12</sup>

The majority of CAR T cell work to date has used viral vectors to produce constitutively expressed CAR molecules.<sup>13</sup> However, CARs may also be introduced into T cells using in vitro transcribed mRNA,<sup>14</sup> and we have shown that effective CAR T cells can be made using the same innovations that enabled mRNA COVID-19 vaccine development.<sup>15,16</sup> Using mRNA to generate CAR T cells may offer several advantages. First, mRNA transfection is a more efficient process than viral transduction, resulting in uniformly high cell surface levels of CAR.<sup>17</sup> Second, due to the quicker production time, iterative changes in the CAR binding site or structure can be more easily tested.<sup>18</sup> Third, mRNA is less expensive than viral vectors when scaling up to clinical grade application. Finally, when exploring novel immunotherapeutic targets, the transient expression of mRNA may be desirable to ensure safety, particularly in the brain where both on-tumor and on-target/off-tumor toxicity may cause significant morbidity and mortality.<sup>19,20</sup> Prior studies using virally transduced CAR T cells in pontine and thalamic murine brain tumor models resulted in toxic death of animals from swelling and herniation,<sup>21</sup> highlighting the need for controlled CAR T cell activity in the brain. The major disadvantage of using mRNA CAR T cells is the transient nature, which may not offer the persistence needed for full eradication of disease,<sup>18</sup> but may be addressed by repetitive dosing of a fully human CAR construct. Prior work has shown that while systemic delivery of mRNA CAR T cells does not result in long-term disease control,<sup>22–24</sup> local delivery into solid tumors can be remarkably effective.<sup>25,26</sup>

We have recently shown that glypican 2 (GPC2), a heparan sulfate proteoglycan oncoprotein, is overexpressed on the surface of neuroblastomas as well as several other pediatric and adult cancers.<sup>27,28</sup> GPC2 appears to harbor key qualities of an immunotherapeutic target: cell-surface location, tumor-specific expression, tumor dependence, and enrichment in the tumor stem cell compartment.<sup>27,28</sup> We and others have identified several GPC2-specific binders<sup>27,29,30</sup> and shown robust efficacy of GPC2-targeting antibody–drug conjugates (ADCs),<sup>27,28</sup> immunotoxins,<sup>29</sup> and DNA vector-derived

CAR T cells.<sup>29,30</sup> Here we sought to build on these data by focusing on GPC2 in pediatric brain cancers, with the goal of better defining the brain tumor histotypes that harbor high levels of GPC2 expression and the genomic biomarkers correlated with high GPC2 expression, as well as creating GPC2-directed mRNA CAR T cells.

## METHODS

### RNA sequencing of primary tumor samples and patient-derived xenografts

RNA sequencing (RNAseq) of pediatric brain tumor samples was completed as described within the Pediatric Brain Tumor Atlas (OpenPBTA; available at <https://alex-slemonade.github.io/OpenPBTA-manuscript/v/0d99c02483e21557e27957386d419b58fe8cb635/> or from the public CAVATICA project: <https://cavatica.sbgenomics.com/u/cavatica/openpbta>).<sup>31</sup> Briefly, 1028 paired-end RNA fastq files, comprising 970 rRNA-depleted and 58 poly-A enriched samples, were aligned to the hg38 human genome using GENCODE V.27 as reference annotation with STAR V.2.6.1d. For comparison with neuroblastoma, data from TARGET (<https://ocg.cancer.gov/programs/target/data-matrix>) were also analyzed. Gene level quantification in terms of transcripts per million (TPM) was quantified using RSEM V.1.3.1. The rRNA depleted and poly-A enriched samples were batch corrected using the ComBat function of R package *sva*.

### Tumor cell lines

Neuroblastoma cell lines were maintained in culture as previously described.<sup>27,32</sup> Brain tumor cell lines were maintained in serum free culture, using DMEM:F12 media supplemented with EGF, FGF, and B27. Luciferase was introduced into pediatric brain tumor cell lines using lentiviral plasmids: pLenti CMV Puro LUC (gift from Eric Campeau and Paul Kaufman,<sup>33</sup> Addgene plasmid #17477; <http://n2t.net/addgene:17477>; RRID:Addgene\_17477) and pLL-EF1a-rFLuc-T2A-GFP-mPGK-Puro (System Biosciences). Preparation and transduction was completed as previously described<sup>27</sup> or with premade lentivirus expressing firefly luciferase with GFP (Cellomics). Cell lines were tested for mycoplasma and confirmed with STR sequencing.

### T cell expansion and transfection

Human T cells from healthy deidentified donors were purchased from the University of Pennsylvania Immunology Core and stimulated with CD3/CD28 beads (Gibco) as previously described.<sup>34</sup> Transfection was completed using Amaxa Nucleofector (Lonza) or ECM 830 (BTX) electroporation systems as previously described.<sup>15</sup>

### CAR construct cloning

Sequences encoding the D3 single chain variable fragment (scFv) were combined with a CD8 hinge and transmembrane domain, followed by 41BB and CD3ζ

costimulatory domains, to create the CAR constructs. CAR plasmids were generated by GenScript, and then cloned into a pTEV vector backbone using Geneart Seamless cloning (Invitrogen).

In vitro mRNA synthesis mRNA encoding CAR constructs were synthesized from the pTEV vectors using Megascript T7 transcription kit (Invitrogen), replacing UTP with 1-methylpseudouridine triphosphate (TriLink Biotechnologies) as previously described.<sup>15</sup> After synthesis, all mRNA was purified with RNase III (Epicenter), followed by capping and tailing as previously described.<sup>15</sup>

### Western blot validation of protein expression

Tumor cell lines were lysed, and western blotting was completed as previously described,<sup>27</sup> using anti-Glypican-2 (1:500; F-5, Santa Cruz Biotechnology) for protein detection.

### Flow cytometry

Flow cytometry was performed on tumor cell lines to confirm cell surface GPC2 expression. Cell lines were washed in FACS buffer (500 mL PBS, 10 mL FBS, 2 mL 0.5 M EDTA), then incubated in D3-GPC2-IgG1 conjugated to phycoerythrin (PE) (Abcam) at 1:800 for 20 min in the dark at 4°C. For quantification of surface GPC2, BD Quantibrite beads (BD Biosciences) were used per manufacturer's instruction.

CAR T cell constructs were evaluated for GPC2-specific binding by staining with GPC2 protein (R&D) conjugated to PE (Abcam). CAR T cells were washed in FACS buffer and incubated in GPC2-PE at 1:100 for 20 min in the dark at 4°C, and then washed again in FACS buffer before analysis. CAR T cells were evaluated for CAR expression on the surface by flow cytometry with protein L (1:100; Genscript) as previously described.<sup>35</sup> Flow cytometry for negative checkpoint regulators was performed as previously described<sup>15</sup> using antibodies: BV510 mouse anti-human CD279 (PD1) (1:100; BD Horizon), PerCP-eFluor 710 mouse anti-human CD223 (LAG-3) (1:100; Invitrogen), and BV421 mouse anti-human CD366 (TIM-3) (1:100; BD Biosciences).

Flow cytometry data were acquired on BD Accuri C6 (BD Biosciences) or FACS Verse (BD Biosciences) flow cytometers. Analysis was completed on FlowJo V.10.2 (Treestar).

### Cytotoxicity assays

Measurement of CAR T cell-dependent tumor cell killing was measured by several methods. For adherent tumor cell lines, cell proliferation was measured every hour using the Real-time Excelligence system (RT-CES; F Hoffman La-Roche). For suspension cell lines, luciferase containing tumor cells were plated in 96-well plates and CAR T cells were added after 24 hours. Bright Glo luciferase assay (Promega) was run after 48 hours of coincubation. CAR T cells were plated in at least triplicate on tumor cells at effector-to-target ratios (E:T) of 10:1, 5:1, and 1:1. Each experiment was

repeated at least two times, with at least two different T cell donors.

### CAR T cell cytokine release

Tumor-specific CAR T cell cytokine release was determined using ELISA to detect interferon-gamma (IFN $\gamma$ ) and interleukin 2 (IL-2). Tumor cells and CAR T cells were plated as described previously and allowed to coincubate for 24–48 hours. Plates were then spun and supernatant collected for evaluation using human IL-2 duoset ELISA (R&D) and human IFN-gamma duoset ELISA (R&D) per manufacturer's instructions.

### Mouse studies

In vivo studies were completed in mice under an approved protocol by the Institutional Animal Care and Use Committee of the Children's Hospital of Philadelphia (CHOP) (IAC 19-000907). Studies used NOD-SCID- $\gamma$ c $^{-/-}$  (NSG) mice aged 6–10 weeks obtained from Jackson Laboratories or bred in-house under pathogen free conditions.

For medulloblastoma studies, RCMB28 xenograft tumors were provided by Dr Robert Wechsler-Reya, and 7316–4509 was provided by the Children's Brain Tumor Network (CBTN). Medulloblastoma xenografts were implanted stereotactically into the cerebellum of mice using the coordinates from lambda: A/P –2.00 mm, D/V 2.00 mm, M/L –2.00 mm. For thalamic diffuse midline glioma (DMG) model, 7316–3058 was provided by the CBTN. This model was injected into the thalamus using the coordinates from bregma: A/P –1.00 mm, D/V 3.50 mm, M/L –0.80 mm. Following engraftment, indwelling catheters for intratumoral CAR T cell delivery were introduced using 26-gauge guide cannulas (P1 Technologies), stereotactically placed and secured to the skull using screws (P1 Technologies) and acrylic resin (Ortho-Jet, Lang). Catheters were placed at the same coordinates as the tumor cell placement. T cells were infused using 33-gauge internal cannulas (P1 Technologies) placed into the guide cannula and delivered over 1 min in a Hamilton syringe. All studies included 6–10 animals per arm and were repeated at least once to confirm results.

### Tissue microarrays

A tissue microarray (TMA) containing normal pediatric tissue from 48 children with non-cancer pathologies was obtained from the Research Institute at Nationwide Children's Hospital (Columbus, Ohio, USA). Tissue types included aorta, adipose, bladder, breast, cartilage, cervix, colon, connective tissue, diaphragm, epididymis, heart, kidney, liver, lung, mesentery, ovary, pancreas, small intestine, skeletal muscle, smooth muscle, spleen, testes, thymus, thyroid, tonsil, trachea and skin. The pediatric high-grade glioma (HGG) tumor TMA from CHOP included primary tumor samples from 73 HGGs (glioblastomas, anaplastic astrocytomas, and DMG), 6 central nervous system (CNS)

embryonal tumors not otherwise specified (NOS), 4 medulloblastomas, 3 pineoblastomas, 2 embryonal tumors with multilayered rosettes (ETMR), 2 ependymomas, 2 atypical teratoid/rhabdoid tumors (ATRT), 1 high-grade neuroepithelial tumor with BCOR alteration (HGNET-BCOR), 1 oligodendroglioma, and 1 low-grade glioma (LGG). The pediatric brain tumor TMAs from the University of British Columbia (BC) included primary tumor samples from the Children's Oncology Group with 9 ATRTs, 13 HGG, 20 ependymoma, and 64 medulloblastoma. Each tissue or tumor type was represented by two to three cores when possible.

### Immunohistochemical analysis

Formalin-fixed, paraffin-embedded TMA sections were analyzed for *GPC2* expression at both CHOP and BC using *GPC2* antibody (Santa Cruz). At CHOP, staining was performed on a Bond Max automated staining system (Leica Biosystems) using the Bond Refine polymer staining kit (Leica Biosystems).<sup>27</sup> At BC, tissue sections were incubated in Tris EDTA buffer (cell conditioning 1; CC1 standard) at 95°C for 1 hour to retrieve antigenicity, followed by incubation with *GPC2* antibody at 1:100 for 1 hour. Intensity scoring was performed on a common four-point scale: 0: no staining, 1: low but detectable degree of staining, 2: clearly positive staining, and 3: strong staining. Expression was quantified as H-Score, the product of staining intensity and % of stained cells. TMA scoring included both tumor and stromal cells. TMAs were scored by two methods to ensure accurate results including a blinded pathologist (one at CHOP, one in British Columbia) and Aperio RUO Image Analysis by Aperio ImageScope. Photographs were taken using a Leica DM4000B.

Xenograft animals treated with CAR T cells had tumors excised and were also stained with *GPC2* (Santa Cruz), H&E, human nuclei stain (Abcam), and human CD3 (Dako) per protocol: [https://www.research.chop.edu/sites/default/files/web/sites/default/files/pdfs/Antibody\\_Protocols.pdf](https://www.research.chop.edu/sites/default/files/web/sites/default/files/pdfs/Antibody_Protocols.pdf). Photographs were taken using a Leica DM4000B.

### Statistical analysis

All data generated were evaluated using Prism V.8 (GraphPad). Comparison of groups for *GPC2* expression was completed using two-sided Mann-Whitney test or Kruskal-Wallis test. Correlation was calculated using two-tailed Pearson. Comparison of means for in vitro and in vivo CAR data were completed using two-sided Student's t-test and two-way analysis of variance. P values <0.05 were considered statistically significant. Data are generally presented as the mean±SD or as noted. Number of samples or replicates is indicated in the results, figures, and figure legends.

## RESULTS

### *GPC2* is expressed in multiple pediatric brain tumors and correlated with *MYCN* expression and chromosome 7q gain

To better define *GPC2* expression in pediatric brain tumors, we analyzed RNAseq data from 20 unique pediatric CNS tumor types (total n=833) in the OpenPBTA dataset, which revealed that several pediatric CNS tumors harbor high levels of *GPC2* (figure 1A). The range of *GPC2* expression levels were similar to other positive cancers we have shown previously such as neuroblastoma<sup>27</sup> and small cell lung cancer (SCLC).<sup>28</sup> Based on normal expression data from the Genotype-Tissue expression portal, we chose a cut-off value of 10 TPM to delineate high *GPC2* expression. Normal tissues have a median TPM well below 10 (median 0.43–4.65 TPM), apart from testes and skin (median TPM 32 and 11, respectively) as previously described.<sup>27</sup> Evaluation of tumors throughout the OpenPBTA biorepository showed high *GPC2* expression in 100% of ETMRs, 95% of medulloblastomas, 93% of other CNS embryonal tumors (CNS embryonal tumor, NOS), 50% of choroid plexus carcinomas (CPC), 41% of HGG without H3K28M mutation, and 40% of DMG (figure 1B). While several tumor histotypes were uniform in their *GPC2* expression levels, multiple subtypes had significant heterogeneity in *GPC2* expression motivating us to look in more detail at *GPC2* expression across tumor molecular subgroups where possible. Embryonal brain tumors showed more uniform high *GPC2* expression with median TPMs greater than 25: ETMR (median TPM 66.64, n=6), CNS NB-FOXR2 (median TPM 139.2, n=2), CNS HGNET-MN1 (median TPM 28.61, n=1), and embryonal tumor NOS (median TPM 57.52, n=12). For medulloblastomas, we observed the highest *GPC2* expression in group 4 compared with the other groups (Wnt, SHH, and group 3; p<0.01) (figure 1C, left), confirming our prior results.<sup>27</sup> Across HGG subgroups, H3G35 mutant gliomas had the highest *GPC2* expression (median TPM 52.33, p<0.05; figure 1C, right).

We have also previously found significantly higher levels of *GPC2* expression in neuroblastoma and medulloblastoma tumors that harbor high expression of a *MYC* gene family member or somatic gain of the *GPC2* locus on chromosome 7q22.<sup>27</sup> To determine if similar drivers of *GPC2* expression are present across this diverse set of pediatric brain tumors, we stratified tumors by chromosome 7q copy number and found that 10% of tumors had 7q gain (38 of 378 tumors with copy number data available). The majority of those were medulloblastoma (14 of 43), LGG (8 of 59), and HGG (8 of 84) (figure 1D). In general, tumors with 7q gain showed significantly higher *GPC2* expression (p<0.01; figure 1E, left). This correlation was also found in medulloblastomas (p<0.01) (figure 1E, center), and a similar trend between 7q neutral and 7q gain in HGG although not statistically significant (figure 1E, right). We also observed a positive correlation between *GPC2* and *MYCN* expression within the dataset (r=0.3073, p<0.0001; figure 1F, left), suggesting that *MYCN* may also transcriptionally regulate

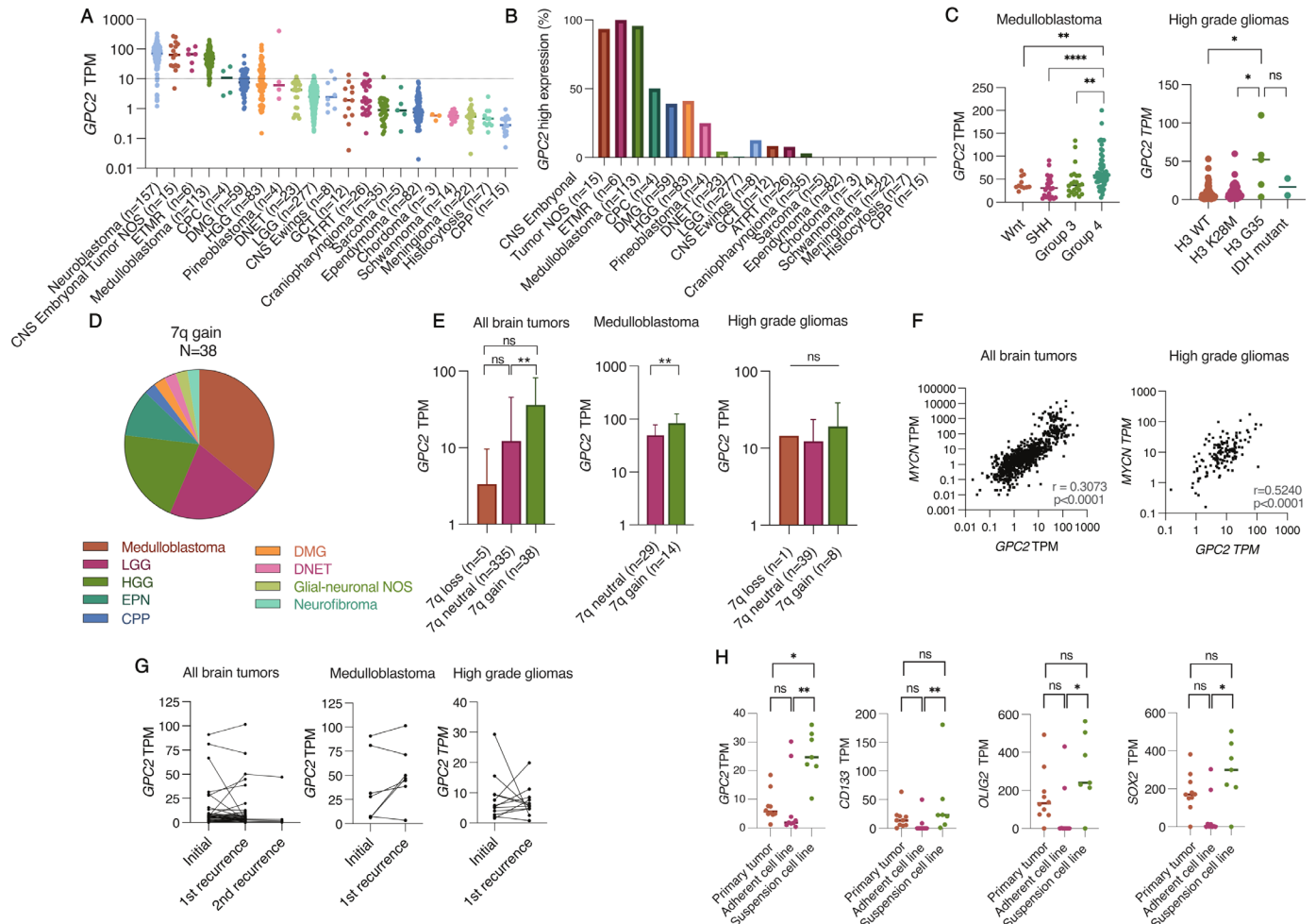


**Figure 1** *GPC2* is expressed in pediatric brain tumors. (A) *GPC2* RNA sequencing data across OpenPBTA pediatric brain tumors cohorts. Neuroblastoma *GPC2* RNA sequencing included for comparison on the left. (B) Using a cut-off value of 10 TPM, percentage of tumors in the OpenPBTA dataset with high expression of *GPC2*. (C) RNA sequencing of *GPC2* expression in medulloblastoma and high-grade glioma subtypes. (D) Summary of tumor histotypes with chromosome 7q gain. (E) *GPC2* expression stratified by chromosome 7q status. (F) Pearson correlation of *MYCN* and *GPC2* expression across all pediatric brain tumor samples (left) and high-grade gliomas (right). (G) *GPC2* expression at primary diagnosis and recurrence across all pediatric brain tumors (left), medulloblastomas (middle), and high-grade gliomas (right). (H) *GPC2*, *CD133*, *SOX2*, and *OLIG2* expression from primary tumor-derived adherent (FBS) or suspension cell lines (serum free media). Individual cases indicated by dots, median indicated by line in A, C, and H. Data in figure part E displayed as mean with SD. \*\*\*\* $P < 0.0001$ ; \*\* $p < 0.01$ ; \* $p < 0.05$ ; ns, not significant. ATRT, atypical teratoid rhabdoid tumor; CNS, central nervous system; CPC, choroid plexus carcinoma; CPP, choroid plexus papilloma; DMG, diffuse midline glioma; DNET, dysembryoplastic neuroepithelial tumor; ETMR, embryonal tumor with multilayered rosettes; GCT, germ cell tumor; HGG, high-grade glioma; LGG, low-grade glioma; NOS, not otherwise specified; TPM, transcripts per million.

*GPC2* expression in some pediatric brain tumors similar to neuroblastoma. The *MYCN/GPC2* correlation was most robust in HGGs ( $r = 0.524$ ,  $p < 0.0001$ ; figure 1F, right) but was not found in medulloblastoma ( $r = 0.16$ ,  $p = ns$ ). *MYC* expression also showed a weak positive correlation with *GPC2* expression across all brain tumors ( $r = 0.21779$ ,  $p < 0.0001$ ) and combined *MYCN* and *MYC* expression for all tumors also correlated with higher *GPC2* expression ( $r = 0.3351$ ,  $p < 0.0001$ ).

To determine if *GPC2* expression is maintained at the time of brain tumor relapse, we evaluated 47 unique patients with paired diagnosis-relapse tumor RNAseq data, including seven patients with multiple relapsed tumor specimens (figure 1G). *GPC2* expression was similar at

the time of diagnosis and relapses across all brain tumor histotypes with mean *GPC2* TPM 10.61 versus 10.05 ( $p = ns$ ). Looking specifically at medulloblastomas and HGGs, *GPC2* expression was generally stable, although individual cases showed both increases and decreases in *GPC2* expression at the time of relapse (figure 1G, middle and right).

The CBTN has generated cell lines for 10 HGG primary tumors in both serum-free and FBS-containing media, with complimentary RNAseq profiling, providing the opportunity to compare *GPC2* expression in these paired in vitro models.<sup>36</sup> *GPC2* expression was increased in HGG cell lines generated in serum-free conditions ( $p < 0.01$ ; figure 1H). This increase

in *GPC2* expression mirrored the expression trends of other neuronal stem cell markers such as *Olig2*, *SOX2*, and *CD133* (figure 1H), suggesting that serum-free conditions better propagate stem-like cells from tumors<sup>37,38</sup> and that *GPC2* expression may be increased in the HGG stem cell compartment, similar to what we have previously described in neuroblastomas and small cell lung cancers.<sup>28</sup>

Finally, we looked to validate these RNA data by quantifying *GPC2* expression in a subset of pediatric brain tumors using immunohistochemistry (IHC), flow cytometry, and western blot. HGGs showed diverse positive *GPC2* staining by IHC with H-scores ranging from 0 to 270, highlighting the intrinsic tumor heterogeneity (figure 2A,B). Strongest staining occurred in the single H3G35 mutant tumor included in the TMA (figure 2B). In addition, strong *GPC2* staining with H scores >100 were also observed in two of four medulloblastomas, one of two ETMRs, two of three pineoblastomas, one of one HGNET-BCOR, and two of six embryonal tumors NOS (figure 2A,C). We also validated our findings using the brain tumor TMA cohort from BC, which showed a similar trend in *GPC2* expression across 13 HGGs, 59 medulloblastomas, 10 ATRT, and 20 ependymomas (figure 2A). Paired *GPC2* IHC staining of a pediatric normal tissue TMA showed very limited normal tissue *GPC2* expression including in heart, kidney, liver, and lung (figure 2A). Corresponding RNAseq data were available for 43 pediatric brain tumor samples and showed a strong correlation between *GPC2* transcripts and protein expression ( $r=0.6324$ ,  $p<0.0001$ ) (figure 2D). To further validate cell surface location of *GPC2*, we performed flow cytometry on medulloblastoma ( $n=4$ ) and HGG ( $n=7$ ) cell lines that confirmed robust *GPC2* cell-surface expression was comparable with the neuroblastoma cell line SMS-SAN (figure 2E,F). Of note, the two cell lines with the highest *GPC2* cell surface expression were derived from a group 4 medulloblastoma (7316–4509) and an H3G35 HGG (7316–158), consistent with transcriptomic profiling and IHC. Finally, total *GPC2* protein expression was quantified in medulloblastoma and HGG cell lines by western blotting and found to be comparable to the SMS-SAN neuroblastoma cell line (figure 2G). Taken together, these data show that *GPC2* is highly expressed on multiple malignant pediatric brain tumors, supporting the testing of *GPC2* immune-based therapies in these lethal childhood CNS tumors.

### mRNA *GPC2* CAR T cells are cytotoxic to *GPC2*-expressing neuroblastoma and brain tumor cell lines

For *GPC2* CAR generation, we used the scFv portion of the D3 *GPC2* antibody, which binds a conformational epitope identical between human and murine proteins of the *GPC2* extracellular domain.<sup>27,28</sup> We explored four configurations of the D3 scFv by manipulating the orientation of the heavy and light chains, as well as the glycine-serine linker length between

the heavy and light chains (5 vs 15 amino acids) (figure 3A). All constructs included a CD8 hinge and transmembrane domain with 41BB costimulatory domain and CD3 $\zeta$  signaling. CAR mRNA was in vitro transcribed and transfected into human T cells, and after 24 hours evaluated for CAR expression and binding to *GPC2*. All four constructs showed *GPC2*-specific binding compared with GD2-directed CAR control (mean MFI 18 721 to 54 849 for constructs vs 684 for control,  $p<0.001$ ) (figure 3B). Serial *GPC2* CAR expression showed that receptors typically persisted for 5–7 days (figure 3C). To investigate T cell exhaustion from potential tonic CAR signaling,<sup>39</sup> we also measured the expression of negative checkpoint regulators on the surface of *GPC2* CAR T cells and found no significant difference in checkpoint molecule expression across the four different constructs (figure 3D).

We next evaluated the cytotoxicity of CAR T cell constructs in vitro using multiple well-characterized neuroblastoma cell lines with variable levels of *GPC2* cell surface expression.<sup>27</sup> T cells transfected with all *GPC2* CAR constructs exerted robust killing of the endogenously *GPC2*-high cell lines SMS-SAN and Nb-EbC1 ( $p<0.0001$ ) (figure 4A). Limited cytotoxicity was observed for CAR constructs D3V2, D3V3 and D3V4 in native SK-N-AS cells, which has overall low but heterogeneous expression of *GPC2* (figure 4B). No off-target killing was observed in control 293 T cells, which have negligible *GPC2* expression (figure 4B). To further validate the specificity of these *GPC2* CARs, we engineered isogenic SK-N-AS via stable lentiviral transduction with forced overexpression of *GPC2* and found that all *GPC2* CAR constructs induced significantly more potent killing ( $p<0.001$ ) (figure 4C). At lower E:T ratios (5:1), there was modest differential cytotoxicity between *GPC2* CARs with the D3V3 and D3V4 constructs performing superiorly, most notable in the NB-EbC1 cell line (figure 4A). Furthermore, there was differential T cell activation across the 4 *GPC2* CARs, with the D3V3 and D3V4 constructs showing the highest levels of IFN $\gamma$  and IL-2 release on coinubation with *GPC2*-high neuroblastoma cells (figure 4D). Considering these data, the D3V3 and D3V4 *GPC2* CAR constructs were prioritized for further testing in brain tumor models based on their superior in vitro cytotoxicity and T cell activation.

We next tested the cytotoxicity of the prioritized D3V3 and D3V4 *GPC2*-directed CARs in a panel of medulloblastoma and HGG cell lines with different levels of *GPC2* expression, using RT-CES assays for adherent cell lines (DAOY, 7316–913, and 7316–5335) and luciferase assays for suspension cell lines (7316–4509, 7316–3058, and 7316–24). *GPC2*-expressing brain tumor cells were selectively killed with *GPC2* CAR T cells, but not the CD19 control CAR T cells at E:T ratios of 5:1 or higher ( $p<0.0001$ ) (figure 5A,B). *GPC2*-directed CAR T cells also showed significant IFN $\gamma$  release in the presence of

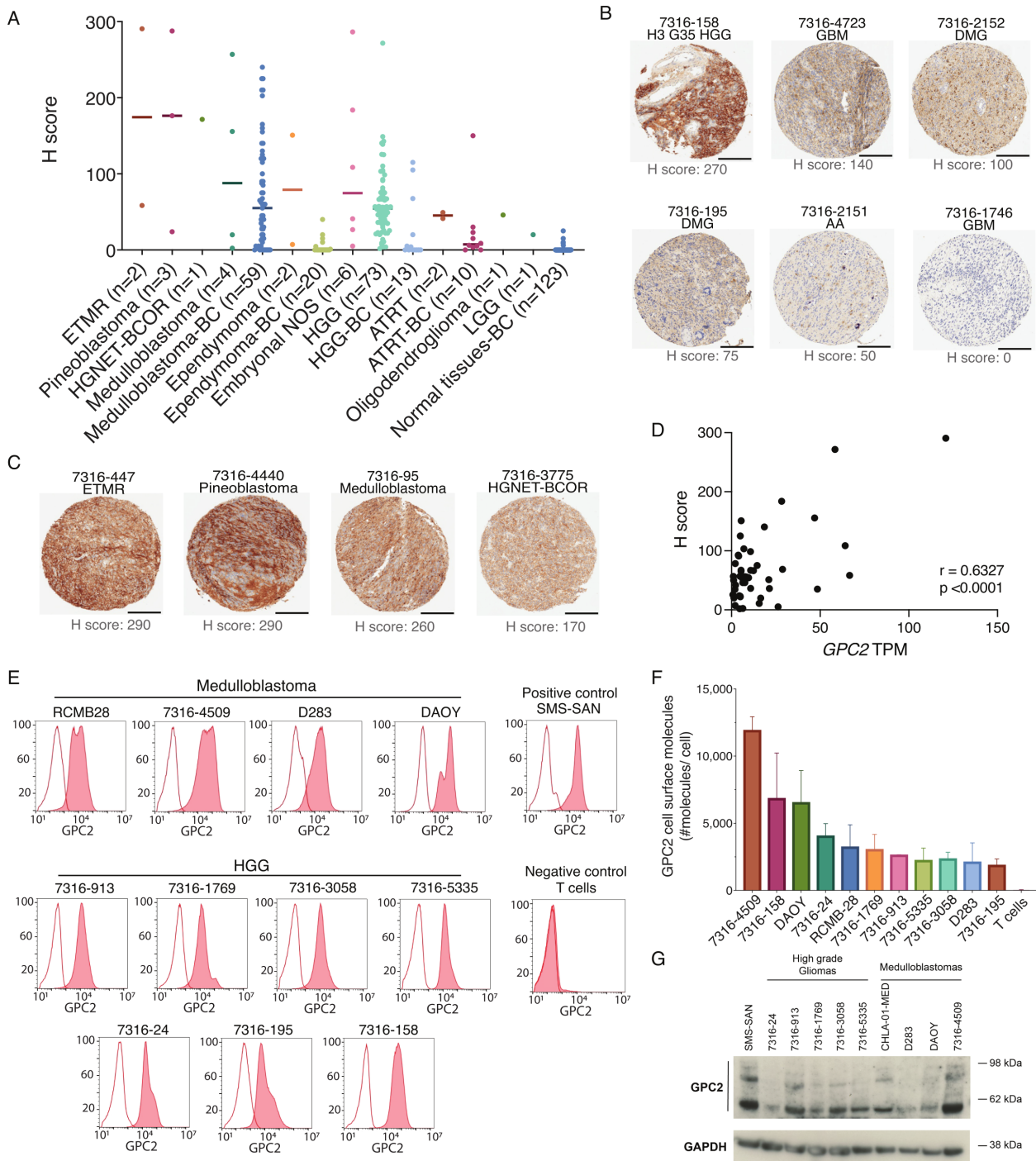


**Figure 2** GPC2 protein is expressed on the surface of pediatric brain tumors. (A) GPC2 H score from IHC of primary brain tumor TMAs. Individual samples indicated by dots, median indicated by line. (B) Representative GPC2 IHC from HGG primary tumor samples including H3G35 mutant HGG, glioblastoma multiforme (GBM), DMG, and AA. Scale bar in black is 200  $\mu$ m. (C) Representative GPC2 IHC showing strongly positive staining in additional brain tumor histotypes including ETMR, pineoblastoma, medulloblastoma, and HGNET-BCOR. Scale bar in black is 200  $\mu$ m. (D) Pearson correlation of *GPC2* RNA expression (TPM) with GPC2 protein expression (H score) from 47 matched pediatric brain tumor samples. (E) GPC2 flow cytometry representative histograms of HGG and medulloblastoma cell lines. Red shaded curves indicate D3-GPC2-IgG1-PE staining, and non-shaded curves indicate isotype control. SMS-SAN shown as neuroblastoma positive control and T cells as negative control. (F) Summary of the relative quantification of GPC2 molecules per cell from flow cytometry of HGG and medulloblastoma cell lines ( $n=11$ ). Data are represented as mean  $\pm$  SD of three independent experiments. (G) GPC2 western blot of a panel of medulloblastoma and HGG cell lines ( $n=9$ ). SMS-SAN also presented as neuroblastoma positive control. AA, anaplastic astrocytoma; ATRT, atypical teratoid/rhabdoid tumors; BC, University of British Columbia; DMG, diffuse midline glioma; ETMR, embryonal tumor with multilayered rosettes; GPC2, glypican 2; HGG, high-grade glioma; HGNET-BCOR, high grade neuroepithelial tumor with BCOR alteration; IHC, immunohistochemistry; NOS, not otherwise specified; TMAs, tissue microarray; TPM, transcripts per million.

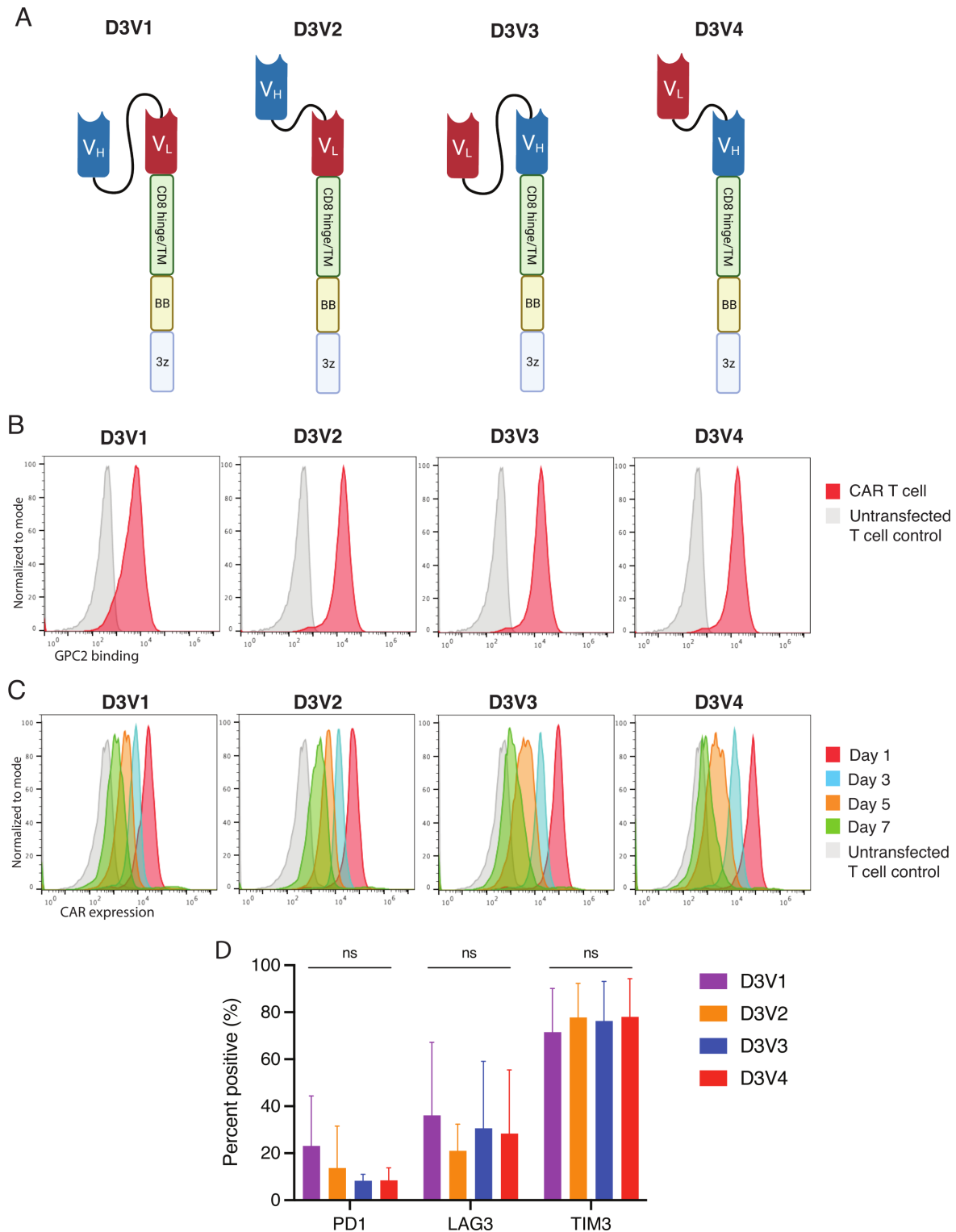


**Figure 3** D3-binder based GPC2-directed mRNA CARs specifically bind GPC2 and are transiently expressed on T cells. (A) Schematic of GPC2 CAR constructs. (B) Flow cytometry representative histograms of GPC2-specific binding by GPC2 CAR T cell constructs. T cells were incubated with GPC2 protein conjugated to PE. Red line is CAR T cell, and gray line is untransfected T cell control. MFI is normalized to mode. (C) Flow cytometry representative histograms of GPC2 CAR persistence on T cells. T cells were incubated with protein L to identify CAR expression. Red line represents day 1 post-transfection, blue line represents day 3, orange line day 5, and green line day 7. Gray line is untransfected T cell control. Mean fluorescence intensity (MFI) is normalized to mode. (D) Cell surface expression of negative checkpoint regulators PD1, Lag3, and Tim3 quantified with flow cytometry at day 4 post-transfection. Data are represented as mean ± SD of five independent experiments. Graphics in figure part A created with BioRender.com. 3z, CD3ζ co-stimulatory domain; BB, 41-BB costimulatory domain; CARs, chimeric antigen receptors; GPC2, glypican 2; ns, not significant; PE, phycoerythrin; T<sub>M</sub>, transmembrane domain; V<sub>H</sub>, variable heavy chain; V<sub>L</sub>, variable light chain.



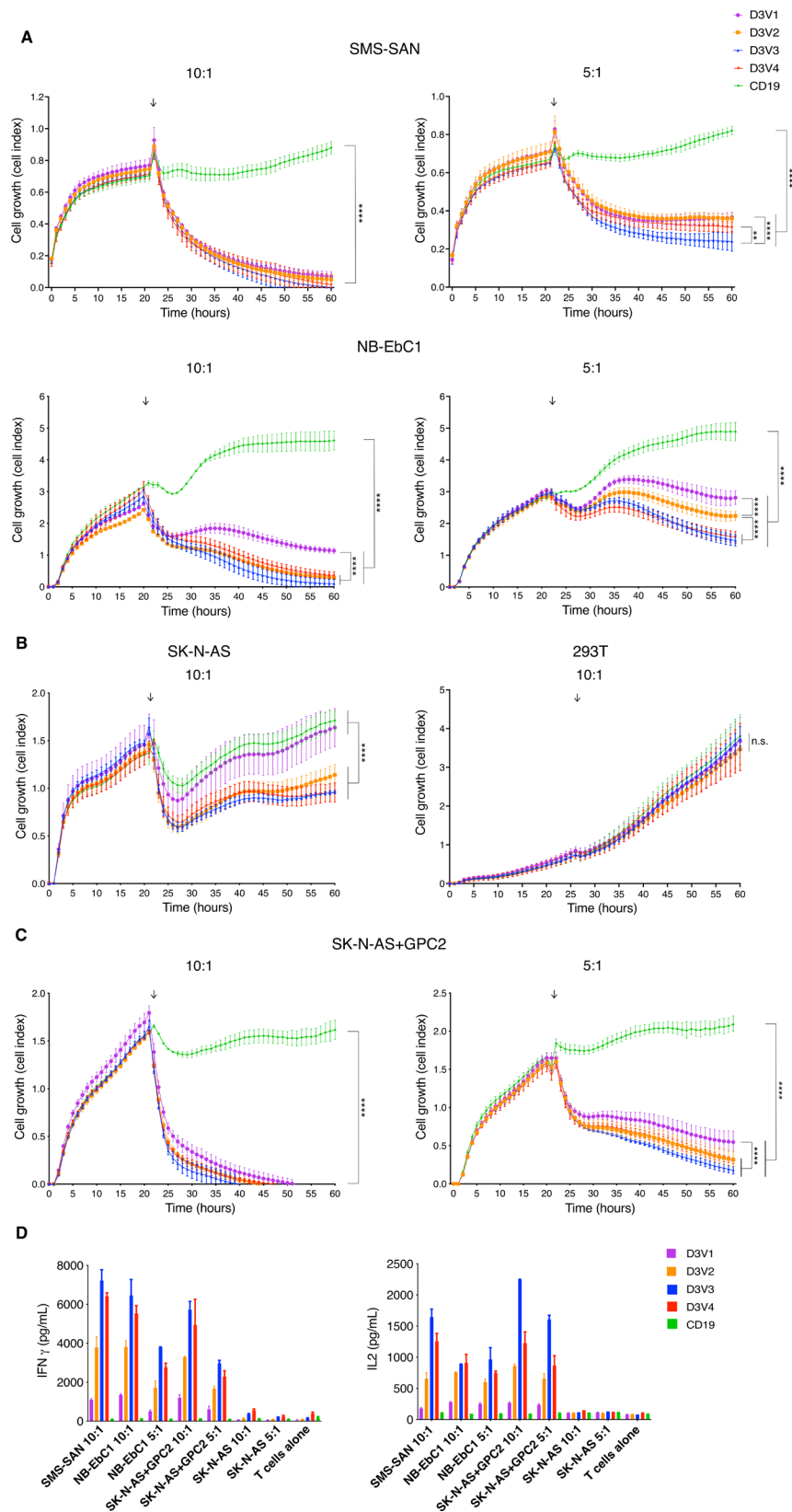


**Figure 4** GPC2-directed CAR T cells produce robust cytotoxicity in neuroblastoma cell line models. (A–C) GPC2-directed CAR T cells coincubated on RT-CES with endogenously high GPC2-expressing neuroblastoma cells lines (A), low/non-expressing cell lines (B), and cell line with forced overexpression of GPC2 (C). T cells added at approximately 24 hours as indicated by arrow. (D) Cytokine expression measured by ELISA 24 hours after coincubation of neuroblastoma and GPC2-directed CAR T cells. Data are shown as mean $\pm$ SD from a representative experiment with each experiment being done two to four independent times. \*\*\*\* $P$ <0.0001; \*\* $p$ <0.01. CAR, chimeric antigen receptor; E:T, effector-to-target ratio; GPC2, glypican 2; IFN $\gamma$ , interferon-gamma; IL-2, interleukin 2; ns, not significant; RT-CES, Real-time Excellence system.

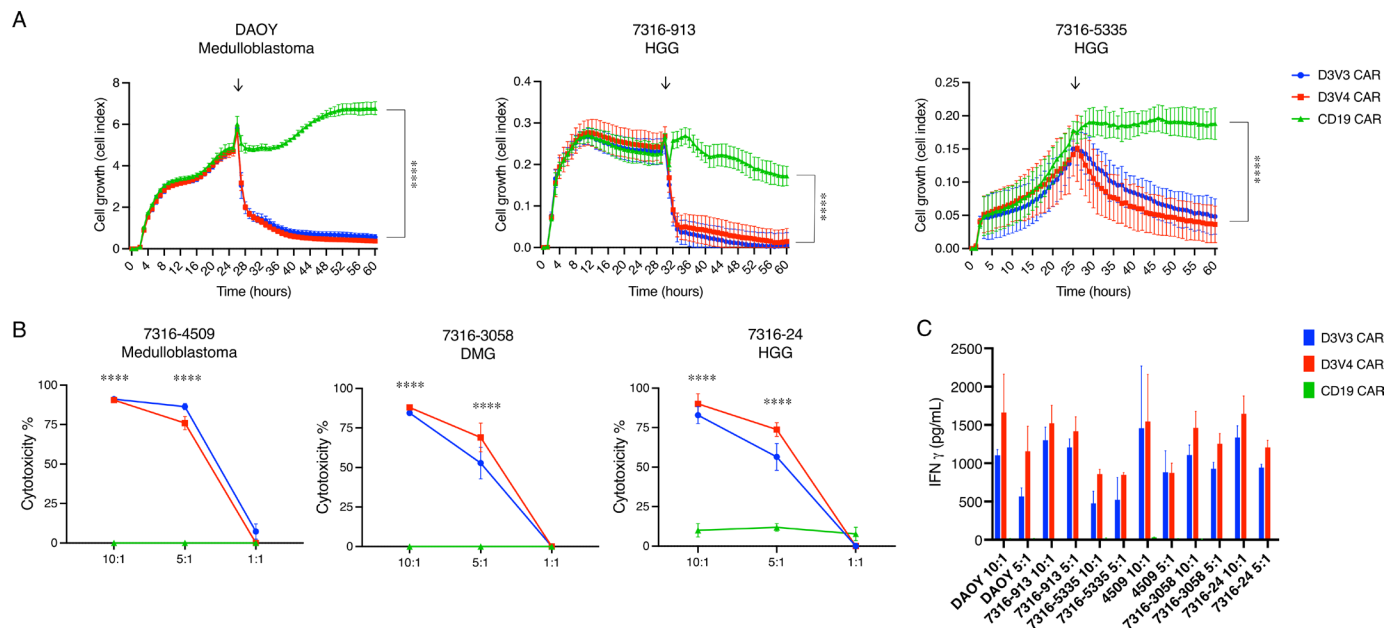


**Figure 5** GPC2-directed CAR T cells produce robust cytotoxicity in pediatric brain tumor cell line models. (A) GPC2-directed CAR T cells coincubated with medulloblastoma (DAOY) and HGG (7316–913, 7316–5335) cell lines. E:T ratio is 5:1, T cells added at approximately 24 hours as indicated by arrows. (B) GPC2 CAR T cells coincubated with medulloblastoma (7316–4509), HGG (7316–24), and DMG (7316–3058) cell lines with cytotoxicity measured using a luminescence assay at 48 hours. (C) Cytokine levels measured 24 hours after coincubation of GPC2 CAR T cells with each cell line. Data are shown as mean $\pm$ SD from a representative experiment with each experiment being done two to four independent times. \*\*\*\* $P$ <0.0001. CAR, chimeric antigen receptor; E:T ratio, effector-to-target ratio; DMG, diffuse midline glioma; GPC2, glypican 2; HGG, high-grade glioma.

GPC2-expressing brain tumor cell lines compared with CD19-directed CAR T cells ( $p$ <0.0001) (figure 5C).

### mRNA GPC2-redirected CAR T cells induce tumor regression and increased survival in pediatric brain tumor xenograft models

To evaluate the efficacy of the D3V3 and D3V4 mRNA GPC2-directed CAR T cells in vivo, we used medulloblastoma and DMG xenograft models. We focused on intratumoral delivery of the mRNA CAR T cells, given the shortened duration of activity with mRNA, and recent work on CAR T cells for CNS tumors reporting increased efficacy with locoregional delivery.<sup>9,40</sup> Following orthotopic tumor engraftment of 7316–4509 group 4 medulloblastoma in mice, we placed a fixed guide cannula into the tumor bed to enable serial CAR T cell dosing. After 14 days with tumor confirmed on bioluminescent imaging, we treated mice with  $4 \times 10^6$  of either GPC2-directed or CD19-directed CAR T cells twice a week for 2 weeks. Both D3V3 and D3V4 CAR T cell constructs resulted in 7316–4509 medulloblastoma tumor regression by day 25; however, only D3V4 CAR T cells produced a durable response showing significant tumor regression at 40 days ( $p$ <0.01; figure 6A). We next treated the group 3 medulloblastoma xenograft RCMB28<sup>41</sup> in an identical manner with  $4 \times 10^6$  of either D3V3 or D3V4 GPC2-directed or CD19-directed CAR T cells twice a week for a total of five doses. Tumor growth was stalled transiently with D3V4 CAR T cells via bioluminescent imaging, but ultimately tumors regrew to similar size as control animals ( $p$ =ns, figure 6B). For both models, tumor presence and regression was also confirmed

by IHC at study endpoint (figure 6C,D). Notably, no evidence of clinical toxicity was observed in these animals other than expected xenogeneic graft-versus-host disease (GVHD)<sup>42</sup> seen in both controls and GPC2-directed treatment groups. There was no neurologic toxicity using the CARs engineered from the D3 GPC2 antibody that binds equally to the murine and human GPC2 protein.<sup>28</sup>

As both the 7316–4509 and RCMB28 medulloblastoma xenograft models developed clinical signs of xenogeneic GVHD from repeated doses of human T cells prior to tumor end point, we next used the aggressive, fast-growing thalamic DMG 7316–3058 xenograft model to evaluate the ability of mRNA GPC2-directed CARs to induce prolonged murine survival. Prior studies treating thalamic DMG xenograft murine models with GD2-directed CAR T cells have resulted in fatal pseudoprogression and hydrocephalus.<sup>21</sup> However, we hypothesized that serial low doses of GPC2 mRNA CAR T cells might avoid CNS toxicity due to their transient nature but still provide tumor control. Using lower doses of  $2 \times 10^6$  GPC2-directed or CD19-directed CAR T cells also allowed study observations up to 60 days postinitial T cell infusion before development of GVHD. CAR T cells were delivered intratumorally via catheter for a total of six doses, and D3V3 and D3V4 GPC2-directed CAR T cells both significantly prolonged murine survival compared with CD19 CAR T cell controls (median survival of 55 days for D3V3 and >60 days for D3V4 vs 33 days for CD19;  $p$ <0.05 and  $p$ <0.01, respectively) (figure 6E). Again, no toxicity was observed during the prolonged course of this study.

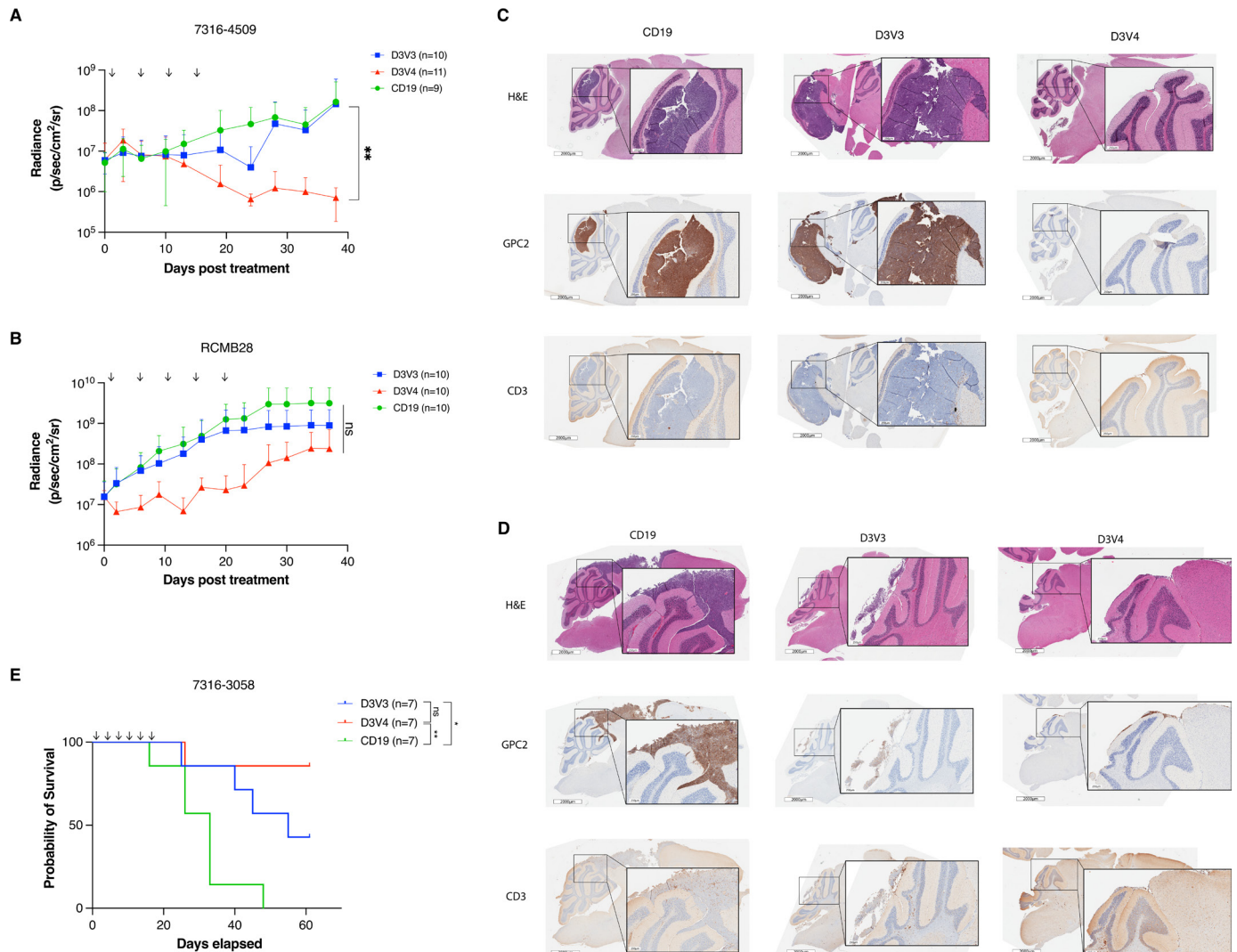


**Figure 6** GPC2-directed CAR T cells mediate antitumor responses and prolong survival in pediatric brain tumors in vivo. (A) Quantification of bioluminescence of the orthotopic group 4 medulloblastoma xenograft 7316–4509 treated with either GPC2 or CD19-directed mRNA CAR T cells. Doses indicated by arrows on graph. Data displayed as mean±SD, n=9–11 mice per arm. (B) Quantification of bioluminescence of the orthotopic group 3 medulloblastoma xenograft RCMB28 treated with either GPC2 or CD19-directed mRNA CAR T cells. Doses indicated by arrows on graph. Data displayed as mean±SD, n=10 mice per arm. (C and D) IHC of murine brains of a representative mouse per group collected at study endpoint from medulloblastoma xenograft experiments using models 7316–4509 (C) and RCMB28 (D). GPC2 staining for tumor identification and expression, CD3 stain to identify CAR T cells. Scale bar is 2000  $\mu$ m at low power, 250  $\mu$ m at insert. (E) Overall survival of mice implanted with thalamic DMG xenograft 7316–3058 treated with six repeated doses of  $2 \times 10^6$  CAR T cells. Doses indicated by arrows on graph. n=7 mice per arm. \*\*\*\*P<0.0001; \*\*p<0.01; \*p<0.05. CAR, chimeric antigen receptor; DMG, diffuse midline glioma; GPC2, glypican 2; IHC, immunohistochemistry; ns, not significant.

## DISCUSSION

Pediatric brain tumors are the leading cause of death in pediatric oncology.<sup>43</sup> Our group recently identified GPC2 as an immunotherapeutic target in neuroblastoma with expression in other pediatric and adult tumors, demonstrating robust and sustained efficacy of a GPC2 ADC using the GPC2 D3 antibody.<sup>27–28</sup> We and others have also shown that viral-based CARs with alternative GPC2 scFvs demonstrate significant efficacy in neuroblastoma murine models.<sup>29–30,44</sup> Here we focus on GPC2 in pediatric brain tumors, both in quantifying GPC2 expression across a wide range of unique brain tumor histotypes and on

developing mRNA-based GPC2-directed CARs to enable pediatric brain tumor treatment approaches.

Investigation of GPC2 expression using RNAseq and various proteomic analyses revealed elevated GPC2 expression across diverse groups of pediatric brain tumors. Many of these tumors have embryonal origins similar to neuroblastoma, such as medulloblastoma, ETMR, CNS embryonal tumors NOS, and pineoblastomas. However, we also observed high GPC2 expression in HGG and CPC. H3G35 mutant tumors showed the highest *GPC2* expression among HGGs and have previously been shown to be driven by MYCN overexpression,<sup>45</sup> potentially consistent

with our findings of MYCN transcriptionally regulating *GPC2* in neuroblastoma and SCLC.<sup>27,28</sup> In fact, across the entire CBTN cohort, *MYCN* and *GPC2* expression were robustly correlated. CPC was also recently shown to be driven by activation of *MYC* paired with loss of TP53.<sup>46</sup> *MYC* expression may also play a role in the regulation of *GPC2*, and future work will focus on understanding factors driving *GPC2* expression in all pediatric brain tumors. These studies also showed that *GPC2* expression is enriched in a malignant stem-like population of HGG tumor cells, consistent with our previous findings of enriched *GPC2* expression in the stem cell compartment of neuroblastomas and SCLCs.<sup>28</sup> Future work will evaluate the potential oncogenic and stem-like properties of these cells in pediatric brain tumors. Importantly, no significant difference in *GPC2* expression was found across diagnosis-relapse paired brain tumor samples, suggesting *GPC2*-directed CARs may be therapeutically efficacious in both settings.

Using mRNA, we developed multiple CAR constructs from one scFv domain, D3, which has been used successfully to create an ADC. Our data showed the light-to-heavy configuration of the scFv proved superior, with best efficacy in vivo using a 5 amino acid linker between the chains. This work was carried out using an mRNA CAR construct for two reasons. First, our mRNA methodology<sup>15</sup> allowed for quick testing and prioritization of the D3V3 and D3V4 constructs and should be used for screening of other novel CAR constructs. Second, mRNA CAR T cells may mitigate potential toxicity when novel CAR T cells are delivered to the brain given their transient CAR expression, which may be particularly relevant for delicate midline structures.

Targeting single antigens with CAR T cells has resulted in antigen escape in clinical trials, particularly in brain tumors where intratumoral heterogeneity is common.<sup>9,47</sup> Indeed, we noted some heterogeneity in *GPC2* IHC staining of several brain tumors on our TMA, and intratumoral heterogeneity also may have been under-represented in the small sample analyzed. As such, targeting *GPC2* alone may result in selection for *GPC2*-negative tumor cell clones and resistance to CAR T therapy. However, conversely, we showed that *GPC2* appears to be expressed on stem-like cells in HGG, and thus targeting this cell population may be especially important in driving durable tumor eradication. Future studies will be aimed at identifying alternative cell surface targets and developing combinatorial CAR T cell targeting to overcome tumor heterogeneity and potential antigen downregulation.

In our studies, *GPC2* expression was retained in murine tumors that progressed or recurred, which may reflect decreased efficacy from the transient mRNA CAR T cells in those tumors. In addition, the differential in vivo efficacy we observed in the medulloblastoma xenografts might be explained by the density of cell surface *GPC2*, as 7316–4509 cells have a significantly higher number of *GPC2* cell surface molecules than RCMB28 cells. Recent

work with distinct but similar *GPC2* DNA retroviral CAR constructs showed that like other solid tumor antigens, more effective *GPC2* CARs can be generated with the utilization of CD28 transmembrane domains, potentially enabling the targeting of brain tumors with more modest levels of *GPC2* cell expression like the RCMB28 medulloblastoma xenograft.<sup>44,48</sup>

mRNA CAR T cells have not been shown to effectively eradicate solid tumors via systemic intravenous injection due to their transient nature.<sup>22</sup> However, intratumoral or local delivery can produce tumor regression,<sup>22,25,26,49</sup> which we have also shown here using mRNA *GPC2*-directed CAR T cells in medulloblastoma and thalamic DMG murine xenograft models. With growing evidence for the effectiveness of locoregional delivery of CAR T cells for brain tumors both preclinically<sup>40,50,51</sup> and in trials,<sup>9,12</sup> the cannula system we developed for repeated CAR T cell delivery serves as an important platform for preclinical CAR T cell testing. The cannulas allow for CAR T cell administration that bypasses the blood–brain barrier, similar to intraventricular reservoirs or convection enhanced delivery catheters, with the former currently being used in ongoing clinical trials for CAR T cells in pediatric brain tumors (NCT03500991, NCT03638167, NCT04185038, NCT04196413, NCT04510051),<sup>11</sup> propelling the translational applicability of this work and providing a clinical platform for future studies in humans.

A limitation of these studies is the inability to define the durability of in vivo efficacy of these CAR constructs given the development of GVHD in our mice, a common finding in preclinical CAR T cell studies using NSG mice and human T cells.<sup>42,52</sup> GVHD development precludes monitoring mice for long periods post CAR T cell infusion for recurrence of disease. Future studies will investigate the efficacy of *GPC2* mRNA CARs in syngeneic murine models of pediatric brain tumors to better assess the durability of antitumor effect, along with interrogation of the host immune system's role in *GPC2* CAR efficacy. Additional potential limitations in the clinical translation of this work include the need for repeated doses. Repeated dosing may produce an immunogenic response when delivered in humans, although this can be mitigated by frequent dosing as previously described,<sup>53</sup> and may be less likely in the setting of our fully humanized binder. The need for repeated dosing will also require a larger number of T cells to be collected and manufactured, which may also be problematic particularly for small children. Current clinical trials in pediatric brain tumors with repeated dosing regimens have not had issues with collecting appropriate CAR T cell quantities,<sup>11,12</sup> but experience in this field is early.

In conclusion, this work has shown that the immunotherapeutic target *GPC2* is highly expressed across a variety of pediatric brain tumors, including malignant embryonal tumors (CNS embryonal tumors NOS, ETMRs, medulloblastomas) and a subset of HGGs and DMGs. Using mRNA we created efficacious CAR constructs from the *GPC2* D3 binder and showed proof-of-concept efficacy in

several pediatric brain tumor preclinical models, laying the foundation for the translation of GPC2 CARs to the treatment of pediatric brain tumors.

#### Author affiliations

- <sup>1</sup>Division of Oncology, The Children's Hospital of Philadelphia, Philadelphia, Pennsylvania, USA  
<sup>2</sup>Department of Pediatrics, University of Pennsylvania Perelman School of Medicine, Philadelphia, Pennsylvania, USA  
<sup>3</sup>Center for Data-Driven Discovery in Biomedicine, The Children's Hospital of Philadelphia, Philadelphia, Pennsylvania, USA  
<sup>4</sup>Department of Bioinformatics and Health Informatics, The Children's Hospital of Philadelphia, Philadelphia, Pennsylvania, USA  
<sup>5</sup>Division of Neurosurgery, The Children's Hospital of Philadelphia, Philadelphia, Pennsylvania, USA  
<sup>6</sup>Department of Pathology & Laboratory Medicine, The Children's Hospital of Philadelphia, Philadelphia, PA, USA  
<sup>7</sup>Department of Pathology & Laboratory Medicine, The University of British Columbia, Vancouver, British Columbia, Canada  
<sup>8</sup>Tumor Initiation and Maintenance Program, NCI-Designated Cancer Center, Sanford Burnham Prebys Medical Discovery Institute, La Jolla, California, USA  
<sup>9</sup>BioNTech SE, Mainz, Rheinland-Pfalz, Germany  
<sup>10</sup>Department of Neurosurgery, University of Pennsylvania Perelman School of Medicine, Philadelphia, Pennsylvania, USA  
<sup>11</sup>Tmunity Therapeutics, Philadelphia, Pennsylvania, USA

**Twitter** Jessica B Foster @FosterJb, Jo Lynne Rokita @jolynerokita and Peter J Madsen @petermadsenmd

**Acknowledgements** This research was conducted using data and samples made available by the Children's Brain Tumor Network and Children's Oncology Group. We would like to thank the patients and families who generously donated their tumor specimens.

**Contributors** Conceptualization: JBF, DMB, ACR, JMM, and KRB. Methodology: JBF, TS, DMB, and KRB. Software: JLR and KR. Data curation: JLR and KR. Formal analysis: JBF. Investigation: JBF, CG, AS, CB, MVL, SNB, PJM, AD, PHS, and DMB. Resources: RJW-R, KK, PHS, ACR, JMM, and KRB. Supervision: DMB, ACR, JMM, and KRB. Funding acquisition: JBF, PBS, ACR, JMM, and KRB. Writing – original draft: JBF. Writing – review and editing: all authors. Guarantor – JBF.

**Funding** Alex's Lemonade Stand Foundation (KRB), Children's Hospital of Philadelphia, Giulio D'Angio Endowed Chair (JMM), Damon Runyon Cancer Research Foundation PST-07-16 (KRB), EVAN Foundation (KRB), Grayson Saves Foundation (JBF), Hyundai Hope on Wheels Young Investigator Award (JBF), Kortney Rose Foundation (JBF), National Institutes of Health NCI K12 CA076931-19 (JBF), National Institutes of Health NCI K08 CA230223 (KRB), National Institutes of Health NCI U54 CA232568 (JMM), National Institutes of Health NCI R35 CA220500 (JMM), and St. Baldrick's-Stand Up to Cancer Dream Team Translational Research Grant SU2C-AACR-DT-27-17 (JMM). The St. Baldrick's Foundation collaborates with Stand Up to Cancer. Research grants are administered by the American Association for Cancer Research, the Scientific Partner of SU2C.

**Competing interests** TS is currently employed by Spark Therapeutics. KK is currently employed by BioNTech and is an inventor on a patent related to use of nucleoside-modified mRNA. DMB is currently employed by Tmunity Therapeutics. JBF, DMB, JMM, and KRB hold patents for the discovery and development of immunotherapies for cancer, including patents related to glypican 2 (GPC2)-directed immunotherapies. KRB and JMM receive research funding from Tmunity for research on GPC2-directed immunotherapies and JBF, DMB, JMM, and KRB receive royalties from Tmunity for licensing of GPC2-related intellectual property. JMM is a founder of both Tantigen Bio and Hula Therapeutics, focused on cellular therapies for childhood cancers, but neither are working on GPC2-directed therapeutics. All other authors have nothing to disclose.

**Patient consent for publication** Not applicable.

**Ethics approval** Not applicable.

**Provenance and peer review** Not commissioned; externally peer reviewed.

**Data availability statement** Data are available in a public, open access repository.

**Open access** This is an open access article distributed in accordance with the Creative Commons Attribution Non Commercial (CC BY-NC 4.0) license, which

permits others to distribute, remix, adapt, build upon this work non-commercially, and license their derivative works on different terms, provided the original work is properly cited, appropriate credit is given, any changes made indicated, and the use is non-commercial. See <http://creativecommons.org/licenses/by-nc/4.0/>.

#### ORCID iDs

Jessica B Foster <http://orcid.org/0000-0002-8001-5960>  
 Jo Lynne Rokita <http://orcid.org/0000-0003-2171-3627>  
 John M Maris <http://orcid.org/0000-0002-8088-7929>

#### REFERENCES

- Couzin-Jankel F. Cancer immunotherapy. *Science* 2013;342:1432–3.
- Almåsbaek H, Aarvak T, Vemuri MC. CAR T cell therapy: a game changer in cancer treatment. *J Immunol Res* 2016;2016:5474602.
- Maude SL, Frey N, Shaw PA, et al. Chimeric antigen receptor T cells for sustained remissions in leukemia. *N Engl J Med* 2014;371:1507–17.
- Fry TJ, Shah NN, Orentas RJ, et al. CD22-targeted CAR T cells induce remission in B-ALL that is naive or resistant to CD19-targeted CAR immunotherapy. *Nat Med* 2018;24:20.
- Gardner R, Finney O, Smithers H, et al. CD19CAR T Cell Products of Defined CD4:CD8 Composition and Transgene Expression Show Prolonged Persistence and Durable MRD-Negative Remission in Pediatric and Young Adult B-Cell ALL. *Blood* 2016;128:219.
- First-ever CAR T-cell therapy approved in U.S. *Cancer Discov* 2017;7:OF1-OF.
- Wagner J, Wickman E, DeRenzo C, et al. CAR T cell therapy for solid tumors: bright future or dark reality? *Mol Ther* 2020;28:2320–39.
- O'Rourke DM, Nasrallah MP, Desai A, et al. A single dose of peripherally infused EGFRvIII-directed CAR T cells mediates antigen loss and induces adaptive resistance in patients with recurrent glioblastoma. *Sci Transl Med* 2017;9:eaaa0984.
- Brown CE, Alizadeh D, Starr R, et al. Regression of glioblastoma after chimeric antigen receptor T-cell therapy. *N Engl J Med* 2016;375:2561–9.
- Brown CE, Badie B, Barish ME, et al. Bioactivity and safety of IL13Rα2-Redirected chimeric antigen receptor CD8+ T cells in patients with recurrent glioblastoma. *Clin Cancer Res* 2015;21:4062–72.
- Vitanza NA, Johnson AJ, Wilson AL, et al. Locoregional infusion of HER2-specific CAR T cells in children and young adults with recurrent or refractory CNS tumors: an interim analysis. *Nat Med* 2021;27:1544–52.
- Majzner RG, Ramakrishna S, Yeom KW, et al. GD2-CAR T cell therapy for H3K27M-mutated diffuse midline gliomas. *Nature* 2022;603:934–41.
- Feins S, Kong W, Williams EF, et al. An introduction to chimeric antigen receptor (CAR) T-cell immunotherapy for human cancer. *Am J Hematol* 2019;94:S3–9.
- Foster JB, Barrett DM, Karikó K. The Emerging Role of In Vitro-Transcribed mRNA in Adoptive T Cell Immunotherapy. *Mol Ther* 2019;27:747–56.
- Foster JB, Choudhari N, Perazzelli J, et al. Purification of mRNA encoding chimeric antigen receptor is critical for generation of a robust T-cell response. *Hum Gene Ther* 2019;30:168–78.
- Pardi N, Hogan MJ, Weissman D. Recent advances in mRNA vaccine technology. *Curr Opin Immunol* 2020;65:14–20.
- Barrett DM, Zhao Y, Liu X, et al. Treatment of advanced leukemia in mice with mRNA engineered T cells. *Hum Gene Ther* 2011;22:1575–86.
- Singh N, Barrett DM, Grupp SA. Roadblocks to success for RNA CARs in solid tumors. *Oncimmunology* 2014;3:e962974.
- Morgan RA, Chinnasamy N, Abate-Daga D, et al. Cancer regression and neurological toxicity following anti-MAGE-A3 TCR gene therapy. *J Immunother* 2013;36:133–51.
- Carroll J. Exclusive: Carl June's Tmunity encounters a lethal roadblock as 2 patient deaths derail lead trial, raise red flag forcing rethink of CAR-T for solid tumors, 2021. Endpoints News [Internet]. Available: <https://bit.ly/3wPYWm0>
- Mount CW, Majzner RG, Sundaresh S, et al. Potent antitumor efficacy of anti-GD2 CAR T cells in H3-K27M\* diffuse midline gliomas. *Nat Med* 2018;24:572–9.
- Singh N, Liu X, Hulitt J, et al. Nature of tumor control by permanently and transiently modified GD2 chimeric antigen receptor T cells in xenograft models of neuroblastoma. *Cancer Immunol Res* 2014;2:1059–70.
- Liu X, Jiang S, Fang C, et al. Novel T cells with improved in vivo anti-tumor activity generated by RNA electroporation. *Protein Cell* 2017;8:514–26.



- 24 Beatty GL, O'Hara MH, Lacey SF, *et al.* Activity of Mesothelin-Specific chimeric antigen receptor T cells against pancreatic carcinoma metastases in a phase 1 trial. *Gastroenterology* 2018;155:29–32.
- 25 Ang WX, Li Z, Chi Z, *et al.* Intraperitoneal immunotherapy with T cells stably and transiently expressing anti-EpCAM CAR in xenograft models of peritoneal carcinomatosis. *Oncotarget* 2017;8:13545–59.
- 26 Beatty GL, Haas AR, Maus MV, *et al.* Mesothelin-specific chimeric antigen receptor mRNA-engineered T cells induce anti-tumor activity in solid malignancies. *Cancer Immunol Res* 2014;2:112–20.
- 27 Bosse KR, Raman P, Zhu Z, *et al.* Identification of GPC2 as an oncoprotein and candidate immunotherapeutic target in high-risk neuroblastoma. *Cancer Cell* 2017;32:295–309.
- 28 Raman S, Buongervino SN, Lane MV, *et al.* A GPC2 antibody-drug conjugate is efficacious against neuroblastoma and small-cell lung cancer via binding a conformational epitope. *Cell Rep Med* 2021;2:100344.
- 29 Li N, Fu H, Hewitt SM, *et al.* Therapeutically targeting glypican-2 via single-domain antibody-based chimeric antigen receptors and immunotoxins in neuroblastoma. *Proc Natl Acad Sci U S A* 2017;114:E6623–31.
- 30 Li N, Torres MB, Spetz MR, *et al.* CAR T cells targeting tumor-associated exons of glypican 2 regress neuroblastoma in mice. *Cell Rep Med* 2021;2:100297.
- 31 Shapiro JA SC, Bethell CJ, Gaonkar KS, *et al.* An open pediatric brain tumor atlas. Manubot [Internet], 2020. Available: <https://alexslomonade.github.io/OpenPBTa-manuscript/v7207b5942e7c5ee8a363f2cc54c4a78ec06f810e/>
- 32 Harenza JL, Diamond MA, Adams RN, *et al.* Transcriptomic profiling of 39 commonly-used neuroblastoma cell lines. *Sci Data* 2017;4:170033.
- 33 Campeau E, Ruhl VE, Rodier F, *et al.* A versatile viral system for expression and depletion of proteins in mammalian cells. *PLoS One* 2009;4:e6529.
- 34 Carpenito C, Milone MC, Hassan R, *et al.* Control of large, established tumor xenografts with genetically retargeted human T cells containing CD28 and CD137 domains. *Proc Natl Acad Sci U S A* 2009;106:3360–5.
- 35 Zheng Z, Chinnasamy N, Morgan RA. Protein L: a novel reagent for the detection of chimeric antigen receptor (CAR) expression by flow cytometry. *J Transl Med* 2012;10:29.
- 36 Ijaz H, Koptyra M, Gaonkar KS, *et al.* Pediatric high-grade glioma resources from the Children's Brain Tumor Tissue Consortium. *Neuro Oncol* 2020;22:163–5.
- 37 Wenger A, Larsson S, Danielsson A, *et al.* Stem cell cultures derived from pediatric brain tumors accurately model the originating tumors. *Oncotarget* 2017;8:18626–39.
- 38 Vik-Mo EO, Sandberg C, Olstorn H, *et al.* Brain tumor stem cells maintain overall phenotype and tumorigenicity after in vitro culturing in serum-free conditions. *Neuro Oncol* 2010;12:1220–30.
- 39 Long AH, Haso WM, Shern JF, *et al.* 4-1BB costimulation ameliorates T cell exhaustion induced by tonic signaling of chimeric antigen receptors. *Nat Med* 2015;21:581–90.
- 40 Theruvath J, Sotillo E, Mount CW, *et al.* Locoregionally administered B7-H3-targeted CAR T cells for treatment of atypical teratoid/rhabdoid tumors. *Nat Med* 2020;26:712–9.
- 41 Ruser JM, Juarez EF, Brabetz S, *et al.* Functional precision medicine identifies new therapeutic candidates for medulloblastoma. *Cancer Res* 2020;80:5393–407.
- 42 Barrett DM, Liu X, Jiang S, *et al.* Regimen-specific effects of RNA-modified chimeric antigen receptor T cells in mice with advanced leukemia. *Hum Gene Ther* 2013;24:717–27.
- 43 Curtin SC, Minino AM, Anderson RN. Declines in cancer death rates among children and adolescents in the United States, 1999–2014. *NCHS Data Brief* 2016;257:1–8.
- 44 Heitzeneder S, Bosse KR, Zhu Z, *et al.* GPC2-CAR T cells tuned for low antigen density mediate potent activity against neuroblastoma without toxicity. *Cancer Cell* 2022;40:53–69.
- 45 Bjerke L, Mackay A, Nandhabalan M, *et al.* Histone H3.3 mutations drive pediatric glioblastoma through upregulation of MYCN. *Cancer Discov* 2013;3:512–9.
- 46 Wang J, Merino DM, Light N, *et al.* Myc and loss of p53 cooperate to drive formation of choroid plexus carcinoma. *Cancer Res* 2019;79:2208–19.
- 47 O'Rourke DM, Nasrallah MP, Desai A, *et al.* A single dose of peripherally infused EGFRvIII-directed CAR T cells mediates antigen loss and induces adaptive resistance in patients with recurrent glioblastoma. *Sci Transl Med* 2017;9. doi:10.1126/scitranslmed.aaa0984. [Epub ahead of print: 19 07 2017].
- 48 Majzner RG, Rietberg SP, Sotillo E, *et al.* Tuning the antigen density requirement for CAR T-cell activity. *Cancer Discov* 2020;10:702–23.
- 49 Schutsky K, Song DG, Lynn R, *et al.* Rigorous optimization and validation of potent RNA CAR T cell therapy for the treatment of common epithelial cancers expressing folate receptor. *Oncotarget* 2015;6:28911–28.
- 50 Donovan LK, Delaidelli A, Joseph SK, *et al.* Locoregional delivery of CAR T cells to the cerebrospinal fluid for treatment of metastatic medulloblastoma and ependymoma. *Nat Med* 2020;26:720–31.
- 51 Brown CE, Aguilar B, Starr R, *et al.* Optimization of IL13R $\alpha$ 2-Targeted chimeric antigen receptor T cells for improved anti-tumor efficacy against glioblastoma. *Mol Ther* 2018;26:31–44.
- 52 Ali N, Flutter B, Sanchez Rodriguez R, *et al.* Xenogeneic graft-versus-host-disease in NOD-scid IL-2R $\gamma$ null mice display a T-effector memory phenotype. *PLoS One* 2012;7:e44219.
- 53 Maus MV, Haas AR, Beatty GL, *et al.* T cells expressing chimeric antigen receptors can cause anaphylaxis in humans. *Cancer Immunol Res* 2013;1:26–31.